

SVM/SVR Kernels as Quantum Propagators

Nan-Hong Kuo¹, Tsung-Wei Chiang², and Renata Wong³

¹Department of Physics, National Taiwan University, Taipei, Taiwan

²Department of Computer Science and Information Engineering, National Chung Cheng University, Chiayi, Taiwan

³Department of Artificial Intelligence, Chang Gung University, Taoyuan, Taiwan

In this work, we establish the equivalence between Support Vector Machine (SVM) kernels and quantum Green's functions. Drawing on the analogy between margin maximization in SVMs and action extremization in Lagrangian mechanics, we show that many standard kernels correspond naturally to Green's functions and that this correspondence arises from the inversion of physical operators. We further demonstrate how positive semi-definiteness, which is essential for valid SVM kernels, aligns with the spectral properties that ensure well-defined Green's functions.

We employ the Kernel Polynomial Method (KPM) to create custom kernels for cases where the commonly employed kernels don't lead to a convergence. These custom kernels approximate the desired Green's functions. We furthermore demonstrate numerically on examples taken from physical problems, such as electrical conductivity, scattering amplitudes, photonic crystals, and energy levels of anharmonic oscillators, that selecting kernel functions that mirror the mathematical form of the associated Green's function can significantly enhance the predictive accuracy of machine learning models.

1 Introduction, Motivation and Background

Support Vector Machines (SVMs) have established themselves as a foundational technique in machine learning due to their robustness in classification and regression tasks [1, 2]. Central to their efficacy is the kernel trick, which implicitly maps input data into high-dimensional feature spaces, enabling the separation of complex, non-linear patterns [3]. Concurrently, quantum mechanics employs Green's functions as fundamental tools to describe the propagation of particles and the response of systems to external perturbations [4].

1.1 Purpose and Contributions of the Paper

This paper provides a rigorous exploration of the mathematical and physical equivalence between SVM kernel functions and quantum Green's functions. Through comprehensive studies on various quantum systems, we demonstrate that selecting kernel functions mirroring the mathematical form of the Green's function associated with a particular physical quantity can significantly improve the accuracy and reliability of machine learning models.

In particular, our contributions include:

- Establishing a mathematical correspondence between common SVM kernels and quantum Green's functions.
- Providing physical interpretations of key theorems, such as Mercer's theorem and the representer theorem, within the context of quantum mechanics.
- Introducing the Kernel Polynomial Method (KPM) as a tool for designing custom kernels aligned with specific quantum systems.

Nan-Hong Kuo: d91222008@gmail.com

Tsung-Wei Chiang: twchiang@cs.ccu.edu.tw

Renata Wong: renata.wong@cgu.edu.tw, corresponding author

arXiv:2502.11153v1 [quant-ph] 16 Feb 2025

- Demonstrating practical applications, including computing electrical conductivity using SVM regression, scattering amplitude calculations, anharmonic oscillator energy level predictions, and photonic crystal modeling.
- Analyzing the limitations of certain kernels, particularly the sigmoid kernel, and proposing modifications to ensure their correspondence with Green’s functions.

1.2 Related works

Research into the relationship between Green’s functions and kernel methods goes back as far as 1974, when Deeter and Gray [5] observed a correspondence between the discrete Green’s function and the Bergman kernel. The Bergman kernel is used for the study of complex structures and their geometric properties, such as curvature and boundary conditions. It has been used in quantum information theory to define a metric on quantum state spaces and is a precursor to the kernels used nowadays in machine learning.

In 1987, Davies [6] studied the equivalence of the heat kernel with the upper and lower bounds of Green’s function. The heat kernel is a solution to the heat equation, which describes the diffusion of particles over time. In quantum field theory, the heat kernel is used to regularize path integrals. In 2022, Fasshauer [7] considered the Radial Basis Function (RBF) and its relation to Green’s functions for differential equations.

Among the most recent approaches, we have Dean et al. [8] who use kernels to describe quantum correlations of N non-interacting spinless fermions in their ground state. Then, they provide a method to compute the kernel in terms of the Green’s function for the corresponding single particle Schrödinger equation. On the other hand, Gin et al. [9] for example use deep learning to learn the Green’s function kernels with the purpose of solving non-linear differential equations. Li et al. [10] do the same for linear partial differential equations.

The literature in the field is limited, and mostly constrained to applications in mathematics. As far as we can tell, all the previous studies were concerned with identifying equivalence relations between single kernels and Green’s functions. In this paper, for the first time, we provide a collec-

tive treatment of the equivalence between Green’s functions and kernel methods with applications in machine learning. We also propose a way to create custom kernels that correspond more closely to particular Green’s functions.

1.3 SVMs and Green’s Functions

Here, we briefly review the essential concepts of Support Vector Machines (SVMs) and quantum Green’s functions required for our subsequent discussions.

1.3.1 Key Elements of SVM Kernel Methods and Quantum Green Functions

Support Vector Machines [1, 2] aim to find a hyperplane that separates data into different classes (or fits a regression function) with maximum margin.

Common kernel functions include:

- **Radial Basis Function (RBF):**

$$K(\mathbf{x}, \mathbf{x}') = \exp(-\gamma \|\mathbf{x} - \mathbf{x}'\|^2) \quad (1)$$

- **Linear Kernel:**

$$K(\mathbf{x}, \mathbf{x}') = \mathbf{x}^\top \mathbf{x}' \quad (2)$$

- **Polynomial Kernel:**

$$(\gamma \mathbf{x}^\top \mathbf{x}' + r)^d \quad (3)$$

- **Sigmoid Kernel:**

$$\tanh(\gamma \mathbf{x}^\top \mathbf{x}' + r) \quad (4)$$

In quantum mechanics, the Green’s function $G(x, x'; E)$ is the inverse of the operator $\hat{H} - E$, where \hat{H} is the Hamiltonian. Physically, G describes how a disturbance at x' propagates to x . In imaginary time, the Euclidean Green’s function $G_E(x, x'; \tau)$ often appears in a Gaussian-like form, such as:

$$G_E(x, x'; \tau) = \left(\frac{m}{2\pi\hbar\tau} \right)^{d/2} \exp \left(-\frac{m(x - x')^2}{2\hbar\tau} \right) \quad (5)$$

where τ is the imaginary time, m is the mass of the particle, d is the spatial dimension, \hbar is the reduced Planck’s constant.

1.3.2 SVM Regression for Predicting Physical Quantities

Although Support Vector Machines are widely known as classification tools, they can also tackle *real-valued* predictions through **Support Vector Regression** (SVR). In this approach, the core optimization shifts from maximizing classification margin to minimizing regression error while preserving a margin-based structure in feature space.

Core Idea. For each physical problem, we extract features \mathbf{x}_i (e.g. wavevectors, angles, potential parameters) and associate them with continuous targets $y_i \in \mathbb{R}$ (such as conductivity or energy). SVR then fits a function

$$f(\mathbf{x}) = \sum_{j=1}^N (\alpha_j - \alpha_j^*) K(\mathbf{x}, \mathbf{x}_j) + b,$$

where K is a kernel function aligned with the system's physical structure (e.g. polynomial for anharmonic expansions, RBF for Gaussian-like behavior, etc.).

We demonstrate how different kernels can address (1) *conductivity* with band-structure features, (2) *scattering amplitudes* via near-linear dependencies, (3) *energy levels* in an anharmonic oscillator, and (4) *photonic* or other periodic systems through custom kernels.

2 Mathematical and Formal Equivalence Between Kernel Functions and Green's Functions

In this section, we explore the mathematical equivalence between SVM kernel functions and quantum Green's functions, highlighting their shared roles in mapping and operator inversion.

2.1 Comparing the Mathematical Forms

The RBF kernel in SVMs, as defined in Eq. (1), and the Euclidean Green's function, as defined in Eq. (5), both exhibit Gaussian dependence on the squared distance between points. By identifying the parameters appropriately, we observe that:

$$\gamma = \frac{m}{2\hbar\tau}, \quad (6)$$

where γ is the kernel parameter in the RBF kernel, m is the mass of the particle, \hbar is the reduced Planck constant, and τ is the imaginary time.

Neglecting the constant prefactor, we have:

$$K(\mathbf{x}, \mathbf{x}') \propto G_E(\mathbf{x}, \mathbf{x}'; \tau). \quad (7)$$

This indicates a direct mathematical equivalence between the RBF kernel and the Euclidean Green's function, suggesting that the RBF kernel can be interpreted as a propagator in a quantum-mechanical context.

On the other hand, mapping $\phi(\mathbf{x})$ in SVMs can be seen as analogous to the quantum state $|\psi(\mathbf{x})\rangle$ in the Hilbert space. In both cases, we have vectors in high-dimensional spaces, in which inner products play a crucial role. In SVMs:

$$K(\mathbf{x}, \mathbf{x}') = \langle \phi(\mathbf{x}), \phi(\mathbf{x}') \rangle_{\mathcal{H}}. \quad (8)$$

In quantum mechanics:

$$G(\mathbf{x}, \mathbf{x}'; t) = \langle \mathbf{x} e^{-i\hat{H}'t/\hbar} | e^{i\hat{H}''t/\hbar} \mathbf{x}' \rangle = \langle \psi(\mathbf{x}, \mathbf{t}) | \psi(\mathbf{x}', \mathbf{t}) \rangle \quad (9)$$

Here, $e^{-i\hat{H}'t/\hbar}$ and $e^{i\hat{H}''t/\hbar}$ represent the evolution operators applied to the bra and ket states, respectively, under potentially different Hamiltonians \hat{H}' and \hat{H}'' . This structure mirrors the kernel formulation in SVMs, where the transformation ϕ maps input data into a higher-dimensional feature space.

Furthermore, the feature mapping in SVMs, which maps data points into high-dimensional feature space, is analogous to the construction of the Green's function in quantum mechanics, where the quantum states undergo time evolution. In both cases, these transformations provide a mathematical framework for evaluating the inner product, capturing the similarity or interaction between two states or data points in their respective spaces.

The inner product between states $|\psi\rangle$ and $|\phi\rangle$ in quantum mechanics is:

$$\langle \psi | \phi \rangle = \int \psi^*(\mathbf{x}) \phi(\mathbf{x}) d\mathbf{x}. \quad (10)$$

This formulation highlights how quantum states interact in Hilbert space, with the integral serving as a measure of their overlap. Similarly, in SVMs, the kernel function represents the inner product in the high-dimensional feature space, capturing the similarity between data points after being mapped via the transformation $\phi(\mathbf{x})$.

In both SVMs and quantum mechanics, computations in high-dimensional spaces are handled implicitly, without explicit mapping taking place:

- In SVMs, the feature mapping $\phi(\mathbf{x})$ into a high-dimensional space is not explicitly computed; instead, computations rely on the kernel function $K(\mathbf{x}, \mathbf{x}')$, which directly evaluates the inner product in the transformed space.
- In quantum mechanics, the path integral formulation evaluates quantum amplitudes by summing over all possible paths that a system can take, thereby encapsulating the contributions from an infinite-dimensional space of paths without explicitly enumerating each path.

This implicit handling of high-dimensional spaces highlights a shared mathematical strategy in both fields, enabling efficient computations that may otherwise have been intractable.

2.2 Formal Equivalence Proof Through Operator Inversion, Mercer's Theorem and Regularization

To claim that an SVM kernel exactly corresponds to a Green's function, one must ensure that the operators governing both objects match in their spectral properties, boundary conditions, and self-adjointness or positivity, in addition to showing similarity in their functional form. To that end, we consider the issue from the viewpoint of operator inversion, where we can systematically incorporate conditions such as Mercer's theorem (positive semi-definiteness), PDE boundary constraints, and eigenfunction expansions. Verifying all these aspects in tandem provides a stronger assertion of equivalence.

In quantum mechanics and PDE theory, the Green's function is defined as the inverse (or resolvent) of the operator governing the system, e.g.,

$$G = (\hat{H} - E)^{-1} \quad \text{or} \quad G = (\hat{L} - \lambda)^{-1},$$

which describes how excitations or waves propagate under a given physical operator. Similarly, in SVMs the kernel matrix (or Gram matrix) plays a role analogous to an operator whose inversion (or regularized inversion) yields the support vector coefficients. This view of both the Green's function and the kernel matrix as objects emerging from the inversion of an operator unifies the

two frameworks, as discussed in more detail in Section 2.2.1.

Then, in Section 2.2.2 we discuss the role of eigenfunction expansions and how they relate to Mercer's theorem. In particular, Mercer's theorem guarantees that any symmetric, positive semi-definite kernel can be expressed as a series expansion in terms of orthonormal eigenfunctions. This expansion closely parallels the eigenfunction expansion of the Green's function of a self-adjoint operator.

2.2.1 Operator Perspective in SVMs and Quantum Mechanics

In this section, we compare label-weighted kernel matrices in SVMs with self-adjoint operators in quantum mechanics, as illustrated in Figure 1. The concept of label weighting is standard in SVM dual forms [1, 2], and inversion of a Hamiltonian operator H is classical in quantum mechanics [33].

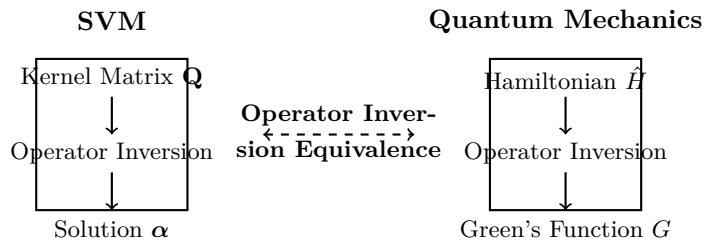


Figure 1: Diagram illustrating the equivalence through operator inversion between SVMs and quantum mechanics. Both require inverting a (positive) operator to obtain the final solution (either α in SVM or G in quantum mechanics).

A key parallel between SVMs and PDE/quantum mechanics is that both rely on inverting a positive (semi-definite) operator to find the final solution. In the SVM dual problem, the relevant operator is the (label-weighted) kernel matrix $\mathbf{Q} = \mathbf{y}\mathbf{y}^\top \circ \mathbf{K}$, where \circ denotes the Hadamard (element-wise) product for incorporating labels \mathbf{y} . Provided that the original kernel matrix \mathbf{K} is positive semi-definite (PSD), \mathbf{Q} is also PSD (up to label sign considerations). Consequently, the support vector coefficients α^* in the dual formulation arise via an effective "inversion" of \mathbf{Q} .

In quantum mechanics or PDE settings, the Green's function G similarly emerges from inverting a self-adjoint operator, such as $\hat{H} - E$ for the Hamiltonian. Figure 1 illustrates this

structural equivalence: SVMs invert \mathbf{Q} to obtain $\boldsymbol{\alpha}$, while quantum/PDE systems invert their Hamiltonian or differential operator to obtain the Green’s function G .

As mentioned previously, a rigorous equivalence between kernels and Green’s functions demands the following conditions are met:

- Eigenfunction expansion: A kernel or Green’s function must expand over orthonormal bases with non-negative eigenvalues.
- Mercer’s theorem vs PDE expansion: A kernel must conform to Mercer’s theorem in order to ensure that it is positive semi-definite. PDE-based Green’s functions rely on self-adjoint operators and suitable boundary conditions in order to have valid solutions.

Once these conditions are met, the kernel and the Green’s function can be shown to be equivalent under appropriate parameterizations and boundary specifications. In what follows, we discuss these two conditions.

2.2.2 Eigenfunction Expansion and Mercer’s Theorem vs. PDE Expansion

Mercer’s theorem [13] originally emerged from the study of integral equations, providing a rigorous mathematical foundation for symmetric positive-definite kernels. The theorem’s relevance for machine learning was established through its application to kernel methods [11, 3]. This connection enabled the use of kernels in SVMs and beyond, thereby pushing forward the field of machine learning by allowing it to embed data into high-dimensional feature spaces without explicitly constructing these mappings (the so-called kernel trick).

As for Green’s functions, the expansion of partial differential equations (PDEs) in terms of eigenfunctions [14] is a cornerstone in classical analysis. Mercer’s theorem and PDE expansion both involve the decomposition of operators into eigenfunctions, with Mercer kernels providing a spectral decomposition similar to the eigenfunction solutions of PDEs.

Both the Mercer expansion for a positive semi-definite kernel and the eigenfunction expansion of a self-adjoint operator’s Green’s function decompose the respective objects into a sum of rank-one contributions. This similarity underscores

the fact that in both cases the underlying eigenvalues and eigenfunctions govern the behavior of the system. Here, we use this observation to build a unifying framework that connects SVM kernel methods with operator inversion in quantum mechanics.

Spectral or Eigenfunction Decompositions
SVM Kernel Operator. According to Mercer’s theorem and standard linear algebra, a symmetric positive semi-definite kernel K can always be expressed as a spectral decomposition:

$$K(\mathbf{x}, \mathbf{x}') = \sum_n \lambda_n \phi_n(\mathbf{x}) \phi_n(\mathbf{x}'), \quad \lambda_n \geq 0. \quad (11)$$

Here, $\phi_n(\mathbf{x})$ are orthonormal eigenfunctions and λ_n are non-negative eigenvalues, representing the spectral components of the kernel.

Green’s Function Operator. In quantum mechanics or PDEs, the resolvent operator $(\hat{H} - E)^{-1}$ associated with a Hamiltonian \hat{H} can similarly be expressed as:

$$G(\mathbf{x}, \mathbf{x}'; E) = \sum_n \frac{\psi_n(\mathbf{x}) \psi_n^*(\mathbf{x}')}{E_n - E}, \quad (12)$$

assuming positivity/resolvent conditions. Here, $\psi_n(\mathbf{x})$ are eigenfunctions of \hat{H} , E_n are the corresponding eigenvalues, and E is the spectral parameter (energy).

Structural Similarity. Both K and G share a common structure: they are sums of rank-1 outer products weighted by spectral coefficients. The kernel K corresponds to a weighted inner product in a high-dimensional feature space, while G represents the propagator in a quantum or PDE system. Under suitable conditions, namely when the domain, boundary conditions, and positivity constraints of the problem coincide, it is possible to establish an isomorphism between the eigenfunction decompositions of the SVM kernel and the Green’s function. In this sense, one may regard K and G as equivalent representations of the same underlying operator inversion (see, e.g., [13, 3, 7] for related discussions).

It is worth noting that while kernel methods rely on integral operators via their Mercer expansions, and PDEs utilize differential operators with eigenfunction expansions, both frameworks ultimately exploit similar spectral properties.

In machine learning, PSD kernel functions serve as the cornerstone of SVMs and kernel

methods. By implicitly mapping input data into high-dimensional feature spaces, kernel functions enable nonlinear separations while satisfying Mercer’s theorem to ensure positive definiteness [3, 11].

Kernel functions can approximate the Green’s functions of PDEs, providing numerical tools for physical modeling. For example: Eq. (11) is analogous to the spectral decomposition of Green’s functions in PDEs, as in Eq. (12). While the mathematical structures are similar, their application backgrounds differ. Kernel functions are primarily used to capture data relationships in high-dimensional spaces, while Green’s functions are fundamental solutions to physical equations.

Positivity and Boundary Conditions.

Mercer’s Theorem for SVM. For $K(\mathbf{x}, \mathbf{x}')$ to be a valid SVM kernel on domain Ω , it must be continuous, symmetric, and *positive semi-definite* (PSD). This ensures a convex SVM dual.

Green’s Function PDE Setup. For $G(\mathbf{x}, \mathbf{x}')$ to serve as an inverse of $(\hat{H} - E)$, we typically require self-adjointness and positivity. Boundary conditions in PDE contexts (Dirichlet, Neumann, etc.) are responsible for the exact form of G . When the domain, boundary conditions, and positivity constraints of an SVM kernel and the corresponding Green’s function are aligned, one can formally establish an equivalence between the two (see, e.g., [13, 7]). Although this is subject to specific assumptions, it serves as a useful guiding principle for designing kernels that reflect the underlying physics.

While common kernels such as the RBF, linear, and polynomial kernels are designed to satisfy Mercer’s condition for all parameter choices, the sigmoid kernel

$$K(\mathbf{x}, \mathbf{x}') = \tanh(\gamma \mathbf{x}^\top \mathbf{x}' + r)$$

does not universally guarantee positive semi-definiteness. Although included as a standard option in many SVM implementations, the sigmoid kernel only meets Mercer’s condition under restrictive parameter regimes (e.g., specific ranges of $\gamma > 0$ and $r < 0$). Outside these regimes, the kernel matrix may lose its PSD property, leading to non-convex optimization or instability in training.

This sensitivity to parameter choices underlines why the sigmoid kernel is less used in prac-

tice than kernels like the RBF that satisfy Mercer’s theorem. This also complicates its use in drawing rigorous parallels between SVM kernels and Green’s functions, since the latter rely on strict positivity and well-defined spectral properties. As a result, while attempting to establish a precise equivalence between SVM kernels and Green’s functions, one must either operate within the safe parameter bounds for the sigmoid kernel or consider alternative kernel choices that inherently satisfy the necessary positivity conditions.

2.2.3 Margin Maximization and Action Extremization

Both SVMs and quantum mechanics involve optimizing a functional. For SVMs, one optimizes the margin through an objective that depends on a kernel K . In quantum and Lagrangian mechanics, one extremizes the action S , which often leads to Green’s functions through operator inversion.

In SVM formulations, the decision hyperplane, which separates classes or fits a regression function, arises from the corresponding optimization problem, which is often solved via its dual formulation:

$$\max_{\alpha} \sum_{i=1}^N \alpha_i - \frac{1}{2} \sum_{i,j=1}^N \alpha_i \alpha_j y_i y_j K(\mathbf{x}_i, \mathbf{x}_j) \quad (13)$$

subject to

$$\alpha_i \geq 0, \quad \sum_{i=1}^N \alpha_i y_i = 0$$

where $K(\mathbf{x}_i, \mathbf{x}_j)$ must be a valid (positive semi-definite) kernel. To handle noise or misclassified samples, one typically adds penalty terms to this objective, leading to a constrained optimization that is solved via Lagrange multipliers.

We can draw a parallel between SVM margin maximization and action extremization in physics. In SVMs, one seeks to maximize the margin by solving a variational problem in a high-dimensional feature space, which leads to a solution expressible as a weighted sum of kernel evaluations. In a similar manner, physical systems are often characterized by the principle of least action, where the trajectory or state of the system is obtained by extremizing a Lagrangian functional. In both cases, the solution is determined by finding a stationary point of an objective functional,

and - in view of the representer theorem - the optimal solution can be represented as a finite linear combination of basis functions (kernel functions in SVMs, or Green's functions in physical systems).

In the context of physical systems, a physical quantity can be derived by defining a Lagrangian

$$\mathcal{L}(\phi(t), \dot{\phi}(t), t),$$

where $\phi(t)$ represents a generalized coordinate describing the state of the system as a function of time t , while $\dot{\phi}(t)$ denotes its time derivative. To obtain the equations of motion, we introduce Lagrange multipliers or enforce the Euler-Lagrange equations with appropriate boundary conditions. For instance, given a Lagrangian:

$$S[\phi, t] = \int \mathcal{L}(\phi(t), \dot{\phi}(t), t) dt, \quad (14)$$

minimizing (or extremizing) $S[\phi], t$ yields the equations of motion for ϕ . The mathematical structure is surprisingly similar to SVM margin maximization: in both cases, one solves for a stationary point of a functional, subject to constraints.

For this reason, we may interpret a physical system's trajectory or field configuration (obtained via the Lagrangian) as analogous to the SVM's decision hyperplane. Determination of the optimal trajectory through a variational principle resembles selecting the optimal hyperplane in SVMs via margin maximization. This perspective allows us to recast certain equations of motion (e.g., in regression or classification tasks) within an SVM framework, particularly when the operator or Green's function governing the physical system is used as the SVM kernel. In the following sections, we expand on these ideas, illustrating how diverse physical quantities can be modeled through a kernel-based approach once the underlying action principle and the associated Green's function are identified.

In addition to the structural equivalence established by operator inversion, the representer theorem guarantees that the solution to a regularized risk minimization problem can be expressed as a finite sum of kernel (or Green's function) evaluations. This further solidifies the connection between SVM methods and physical systems governed by Green's functions.

2.2.4 Link to Equivalence of Regularization Solutions and Green's Functions

While the operator inversion perspective establishes a structural similarity between SVM kernels and Green's functions, it primarily highlights that both arise from inverting a positive (semi-definite) operator. However, this conceptual connection alone does not fully detail how solutions manifest in practice. We discuss the equivalence of regularization solutions to address this gap by providing a constructive framework that complements and extends the operator inversion argument.

A further result, given in Theorem 2.1, states that regularization solutions in PDE/inverse problems can be expanded as sums of Green's functions at data points, mirroring how SVM solutions expand in sums of kernel evaluations. Therefore, the following two points are complementary:

- Recognition of the fact that SVM dual solving $\mathbf{Q}\alpha = \dots$ is analogous to PDE-based Green's function solving $(\hat{H} - E)G = \delta$.
- Equivalence of regularization solutions (Theorem 2.1), which ensures that PDE-based minimizers must lie in the span of Green's functions. This parallels the representer theorem in kernel-based ML and clarifies how both are expansions in the same operator's inverse (assuming positivity, boundary conditions, etc.).

To summarize, while the operator inversion perspective offers a conceptual basis for the equivalence between SVM kernels and Green's functions, Theorem 2.1 and its discussion supplies the detailed constructive link. They validate that solutions obtained via regularization in PDE contexts can be expressed explicitly as expansions in Green's functions, analogous to SVM solutions as sums of kernel evaluations. This constructive equivalence reinforces the operator inversion argument by incorporating spectral positivity, boundary constraints, and functional expansions.

2.3 Formulating Physical Problems as Optimization Problems

Building on the established connection between operator inversion and the equivalence of regular-

ization solutions with Green's functions, we now demonstrate how many physical problems can be reformulated as optimization tasks.

Many problems in physics that involve Green's functions, such as solving PDEs or describing quantum systems, can be reformulated as optimization or variational problems. Consider, for instance, a physical system described by a linear differential operator P (e.g., the Laplace operator). The goal is to determine the physical field $u(x)$ that satisfies certain constraints or fits observed data.

By the representer theorem [3], solutions to regularization problems in a reproducing kernel Hilbert space can be expressed as finite linear combinations of kernel (or Green's function) evaluations at the data points. With this, many physical problems can be cast as minimization tasks over function spaces.

Our particular example can be cast as the following minimization problem:

$$f^* = \arg \min_{f \in H} \left(\sum_{i=1}^N V(y_i, f(x_i)) + \lambda \|Pf\|_{L^2}^2 \right) \quad (15)$$

where:

- $V(y_i, f(x_i))$ is the loss function measuring the discrepancy between the observed value y_i and the predicted value $f(x_i)$,
- $\|Pf\|_{L^2}^2$ is a regularization term controlling the complexity of f , and
- λ is a regularization parameter balancing the trade-off between fitting the data and controlling complexity.

The loss term $V(y_i, f(x_i))$ in the functional resembles the role of a Lagrangian density in physics, where discrepancies between $f(x_i)$ and y_i contribute to the overall "action" that the system seeks to extremize. In this way, the optimization functional parallels a variational principle: just as the Lagrangian integrates over fields and their dynamics to yield equations of motion, the loss term adds up discrepancies to guide the selection of an optimal function f^* . This perspective demonstrates how minimizing such a functional in the context of SVMs or regularization problems is akin to finding a stationary action in physics, thereby providing a direct link between the loss function and physical principles.

On the other hand, this optimization formulation is analogous to finding the optimal decision hyperplane in SVMs, where the goal is to minimize a regularized risk functional. Just as the SVM decision function can be expressed as a sum of kernel evaluations weighted by optimal coefficients (derived from solving a dual problem), the solution f^* here is represented as a combination of Green's functions centered at the data points. This parallel suggests that techniques developed in SVMs can be directly applied to solve complex physical problems.

The Green's function $G(x, x')$, defined as the inverse of the operator P , plays a fundamental role here. By minimizing the above functional, the solution $f^*(x)$ can often be expressed as a linear combination of Green's functions centered at the data points.

In quantum mechanics, the wavefunction $\psi(x)$ is typically obtained by solving the Schrödinger equation, which is inherently a variational problem. Take for example

$$\psi^* = \arg \min_{\psi} \langle \psi | \hat{H} | \psi \rangle \quad (16)$$

subject to $\|\psi\| = 1$, where \hat{H} is the Hamiltonian operator. This optimization minimizes the energy functional and is structurally similar to SVM optimization problems, with the Hilbert space playing the role of the feature space.

In both cases, the minimizer can be expressed in terms of Green's functions, highlighting the intrinsic connection between the two fields.

As discussed above, the link between SVM kernels and Green's functions becomes clearer through the perspective of operator inversion. Both kernel functions $K(x, x')$ in machine learning and Green's functions $G(x, x')$ in physics are solutions to operator-based equations. For SVMs, $K(x, x')$ corresponds to the solution of linear systems involving the kernel matrix \mathbf{K} , which is derived from the inner product in the feature space. For physics, $G(x, x')$ is the inverse of a differential operator, describing how a system responds to a localized perturbation.

In both contexts, the solution can be represented as an inner product in a high-dimensional space, making the representer theorem directly applicable. This mathematical equivalence enables us to replace K with G when solving regularization problems.

We now give a proof in Theorem 2.1 that f^* as defined in Eq. (20) can be expressed as a superposition of Green's functions centered as the datapoints.

Theorem 2.1. *The function f^* minimizing the regularization functional*

$$\mathcal{R}[f] = \sum_{i=1}^N V(y_i, f(x_i)) + \lambda \|Pf\|_{L^2}^2, \quad (17)$$

where P is a linear differential operator, can be expressed as a superposition of Green's functions centered at the data points:

$$f^*(x) = \sum_{i=1}^N \alpha_i G(x, x_i), \quad (18)$$

highlighting the equivalence between the regularization solution and the Green's function.

Proof. By the representer theorem [3] and the properties of the reproducing kernel Hilbert space (RKHS) associated with the operator P , the minimizer of the functional $\mathcal{R}[f]$ lies in the span of the Green's functions $G(x, x_i)$. Specifically, the Green's function $G(x, x')$ of P^*P , where P^* is the adjoint operator of P , satisfies:

$$P^*PG(x, x') = \delta(x - x'), \quad (19)$$

with $\delta(x - x')$ being the Dirac delta function.

Substituting this representation into the functional, it follows that the minimizer $f^*(x)$ can be written as:

$$f^*(x) = \sum_{i=1}^N \alpha_i G(x, x_i), \quad (20)$$

where α_i are coefficients determined by the optimization process. \square

In computational physics, the solution in Eq. (20) arises as the minimizer of a regularization problem involving a linear differential operator P . Specifically, we consider a physical system governed by P and suppose we seek a function $f(x)$ that fits observed data $\{(x_i, y_i)\}_{i=1}^N$ while controlling its complexity. This leads to the minimization problem:

$$\min_{f \in H} \left(\sum_{i=1}^N V(y_i, f(x_i)) + \lambda \|Pf\|_{L^2}^2 \right).$$

By the representer theorem, the solution lies in the span of the Green's functions $G(x, x_i)$ associated with the operator P^*P . For example, in the case of the Poisson equation

$$-\Delta u(x) = \rho(x), \quad x \in \Omega, \quad u|_{\partial\Omega} = 0,$$

the Green's function $G(x, x')$ satisfies

$$-\Delta_x G(x, x') = \delta(x - x'), \quad G(x, x')|_{x \in \partial\Omega} = 0.$$

Then, the regularized solution for approximating $u(x)$ from data $u(x_i) \approx y_i$ can be written as

$$u^*(x) = \sum_{i=1}^N \alpha_i G(x, x_i),$$

which explicitly uses the Green's function of the Laplacian to interpolate and regularize the solution.

In the context of SVMs, the analogous expression

$$f^*(x) = \sum_{i=1}^N \alpha_i K(x, x_i) \quad (21)$$

is derived from solving a regularized optimization problem in a RKHS. Here, the kernel function $K(x, x_i)$ serves a role similar to that of a Green's function, but in the machine learning setting, it implicitly defines a mapping into a high-dimensional feature space.

More concretely, consider a linear differential operator P that maps input data x to a feature space through a transformation $\phi(x)$, i.e.,

$$\phi(x) = Px,$$

where P acts as the linear mapping (or feature extraction operator). The kernel function is then defined as the inner product in the feature space:

$$K(x, x') = \langle \phi(x), \phi(x') \rangle.$$

Using the representer theorem in this RKHS setting, the solution to a regularized risk minimization problem is given by Eq. (21), which mirrors the structure of the physics solution with $G(x, x_i)$. Here, the operator P used to map the input into the feature space is analogous to the differential operator in the physics context. The coefficients α_i are obtained by solving a dual optimization problem, similar to how they are determined in the PDE regularization setting.

Thus, the expressions in Eq. (20) in physics and Eq. (21) in SVMs both represent solutions expanded in terms of Green's functions and kernel functions, respectively, highlighting their equivalence under suitable conditions.

2.3.1 Algorithm: Solving Regularization Problems Using Kernels

Building on Theorem 2.1 and the operator inversion perspective, we present a general algorithm for solving regularization problems by constructing a kernel from a known self-adjoint differential operator P . This approach is widely applicable in computational physics, where P is derived from the governing equations of the system.

Algorithm 1 Solving Regularization Problems with Operator P

Require: Data $\{(\mathbf{x}_i, y_i)\}_{i=1}^N$, differential operator P , regularization parameter λ

Ensure: Function $f^*(\mathbf{x})$

- 1: Compute the Green's function $G(\mathbf{x}, \mathbf{x}')$ satisfying $P^*PG = \delta(\mathbf{x} - \mathbf{x}')$.
- 2: Form the kernel matrix \mathbf{K} with elements $K_{ij} = G(\mathbf{x}_i, \mathbf{x}_j)$.
- 3: Solve the linear system:

$$(\mathbf{K} + \lambda\mathbf{I})\boldsymbol{\alpha} = \mathbf{y},$$

where $\boldsymbol{\alpha} = [\alpha_1, \dots, \alpha_N]^\top$, \mathbf{I} is the identity matrix, and $\mathbf{y} = [y_1, \dots, y_N]^\top$.

- 4: Construct $f^*(\mathbf{x}) = \sum_{i=1}^N \alpha_i G(\mathbf{x}, \mathbf{x}_i)$.
-

This algorithm outlines a general procedure. It begins by computing the Green's function G for the given self-adjoint operator P , establishing the connection to the underlying physical model. Then, using G , a kernel matrix \mathbf{K} is formed, and a regularized linear system is solved to obtain coefficients $\boldsymbol{\alpha}$. And finally, the solution $f^*(\mathbf{x})$ is expressed as a linear combination of Green's functions centered at the data points.

In many practical applications, especially within the scope of Section 3, the Green's function $G(\mathbf{x}, \mathbf{x}')$ corresponding to the physical process is already known from theory or prior computation. In such cases, the initial step of computing G from P can be skipped. The algorithm then simplifies to directly using the known G to form the kernel matrix, solve for $\boldsymbol{\alpha}$, and construct the regression function. This special case is a direct application of the general procedure when the self-adjoint operator P is implicit in the known Green's function.

3 Applications: SVM Regression in Physical Systems

In this section, we consider several aspects of physical systems and how particular kernels perform for these systems. All the examples involve regression using SVMs. SVMs' use for regression is standard [30], with established kernels such as RBF, linear, sigmoid or polynomial [3]. One of the example aspects considered is conductivity, for which we will be using the Kubo formula. Physical modeling of conductivity via the Kubo formula is well-documented; see, for instance, Mahan [31]. In electron-proton scattering, we apply the Born approximation, the description of which can be readily found in standard quantum mechanics references [33].

While the standard kernels are commonly used with SVM, their use and interpretation in alignment with Green's functions are new. Here, we extend this approach to a custom kernel for photonic crystals. Our custom kernel builds on the ideas of domain-specific kernel design [32], with examples of such kernels being periodic kernels, and group-invariant kernels.

Building on the equivalence established between SVM kernels and Green's functions, we now explore various applications of SVM regression in modeling physical systems, demonstrating how aligning kernel functions with corresponding Green's functions enhances predictive accuracy. We examine cases including electrical conductivity, scattering amplitudes, anharmonic oscillator energy levels, and photonic crystals.

3.1 Computing Conductivity Using SVM Regression

Data Acquisition For this example, we used electronic band structures, Fermi levels, and \mathbf{k} -points for copper, which were retrieved from the Materials Project database [29]. Each \mathbf{k}_i corresponds to an electronic energy level ϵ_i in copper's band structure.

Feature Construction The features included group velocities for electronic states, Fermi occupation, and local conductivity contribution, with details as follows:

1. **Velocities** v_i were computed by numerically differentiating the energy bands w.r.t. \mathbf{k}

points, giving the group velocity for each electronic state.

2. **Fermi occupation** $n_F(\epsilon_i)$ was calculated under an assumed temperature T and Fermi level μ ,

$$n_F(\epsilon_i) = \frac{1}{\exp\left(\frac{\epsilon_i - \mu}{k_B T}\right) + 1}. \quad (22)$$

3. **Local conductivity contribution** σ_i was derived from

$$\sigma_i = e^2 v_i^2 n_F(\epsilon_i) \tau, \quad (23)$$

where e is the electron charge, τ is a (constant) relaxation time, and v_i is the group velocity at energy ϵ_i .

We then assembled feature vectors

$$\mathbf{x}_i = [k_{ix}, k_{iy}, k_{iz}, \epsilon_i, n_F(\epsilon_i)],$$

and set σ_i from Eq. (23) as the target variable.

Data Splitting and Normalization The final dataset was split into training and testing subsets (e.g., 80% and 20%). We applied standard scaling (mean subtraction and variance normalization) to stabilize SVM training.

3.1.1 Comparison with the Kubo Formula

The Kubo formula for electrical conductivity is

$$\sigma_{\mu\mu} = \frac{e^2}{\hbar} \sum_{\mathbf{k}} [v_{\mu}(\mathbf{k})]^2 \left(-\frac{\partial n_F(\epsilon_{\mathbf{k}})}{\partial \epsilon_{\mathbf{k}}} \right) \tau. \quad (24)$$

Its emphasis lies in the derivative of n_F near the Fermi level, reflecting that conduction arises from electrons whose occupancy changes significantly with small energy shifts.

By contrast, our SVM-based approach uses the occupancy directly, $\sigma_i = e^2 v_i^2 n_F(\epsilon_i) \tau$, thus omitting the explicit derivative factor in Eq. (24). This simplification can still yield practical, accurate predictions for the system at hand, especially if $n_F(\epsilon)$ varies smoothly or if conduction is dominated by states near the Fermi energy.

3.1.2 Methodology

In the Code Availability section of this work, see `svm_conductivity.py`, we employ **SVR** to perform regression on band-gap and density features, aiming to predict a continuous conductivity value. Because **SVR** is the real-valued extension of SVM. **Kernel Selection.** We tested several kernel functions in SVR (Support Vector Regression):

- *RBF Kernel:* Known for its Gaussian form, often mirroring Green's function structures.
- *Polynomial Kernel:* Introduces polynomial feature interactions.
- *Linear Kernel:* Represents a simple linear hypothesis in feature space.
- *Sigmoid Kernel:* Resembles neural net activation but may fail to ensure positive semi-definiteness under certain parameter settings.

Hyperparameter Tuning We used cross-validation to optimize parameters such as C (regularization), γ (RBF or sigmoid width), and polynomial degree. The best configuration under each kernel was then retrained on the entire training set.

Performance Metrics We used Mean Squared Error (MSE) and the coefficient of determination (R^2) to evaluate predictive accuracy on the test set.

3.1.3 Results and Observations

Figure 2 compares kernel performance in predicting σ_i from real copper data. The RBF kernel outperforms polynomial, linear, and sigmoid kernels, highlighting its aptitude for capturing non-linear, Gaussian-like relationships in electron conduction.

The impressive performance of the RBF kernel indicates that kernels approximating Gaussian or propagator shapes naturally suit electron conduction problems. Furthermore, even though our approach omits the derivative term in Kubo's formula, the kernel delivered strong performance for copper, indicating it may be sufficient when $n_F(\epsilon)$ changes gradually near the Fermi level. Nonetheless, investigating partial-derivative-based features could further refine predictive accuracy.

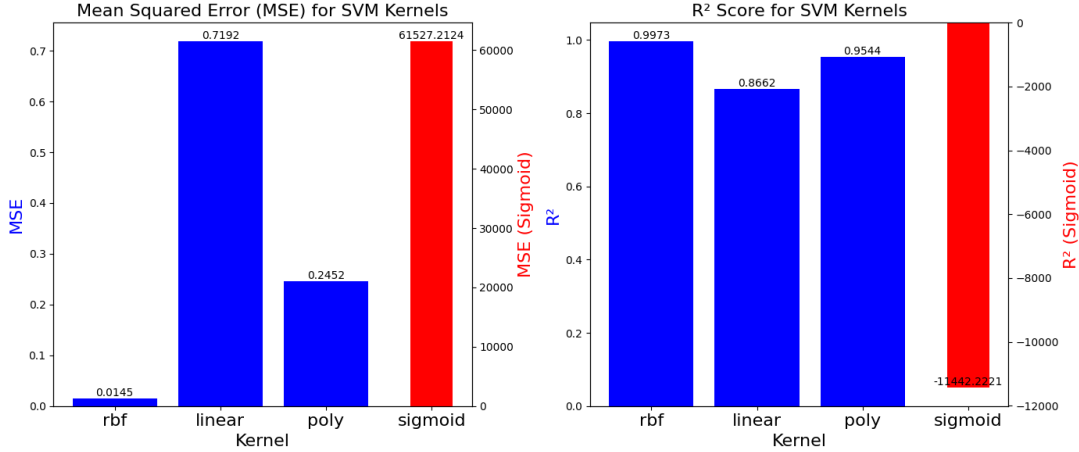


Figure 2: Comparison of SVM kernel performance in predicting electrical conductivity. The RBF kernel performs well in modeling complex non-linearities, reflecting its alignment with the underlying physical (Green’s-function-like) processes. The sigmoid kernel performs poorly due to incompatibilities with these processes.

3.2 Scattering Amplitudes and Linear Kernel

3.2.1 Physical Background

Scattering amplitudes are fundamental quantities in quantum mechanics that describe the probability amplitude of a particle scattering from an initial state to a final state due to an interaction [33]. Understanding scattering processes is crucial in fields like particle physics and condensed matter physics.

In electron-proton scattering, electrons interact with protons via electromagnetic forces. The differential cross-section, which measures the likelihood of scattering at a particular angle, can be derived from the scattering amplitude.

3.2.2 Simulating setup

Dataset Preparation We simulated a dataset representing electron-proton scattering events. Each data point included:

- **Incident Energy** E_i
- **Scattering Angle** θ
- **Scattering Amplitude** $f(E_i, \theta)$

Generating Scattering Data Using the first Born approximation, the scattering amplitude for electron-proton interactions can be expressed as:

$$f(E_i, \theta) = -\frac{me^2}{2\pi\hbar^2} \frac{1}{q^2}, \quad (25)$$

where q is the momentum transfer:

$$q = 2k_i \sin\left(\frac{\theta}{2}\right), \quad (26)$$

and k_i is the incident wave number:

$$k_i = \frac{\sqrt{2mE_i}}{\hbar}. \quad (27)$$

We generated values of E_i and θ within reasonable physical ranges and calculated $f(E_i, \theta)$.

3.2.3 Low-Energy Domain and Code Implementation

The reference file `scattering_linear_kernel.py` for our scattering experiment can be found in Section Code Availability. In it, we consider frequencies in the range $\nu \approx (5 \times 10^{14}) \dots (7 \times 10^{14})$ Hz, focusing on the photoelectric effect near a work function of $\phi = 2.0$ eV. In this low-energy regime, the scattering/emission process is adequately described by a simple *linear* relationship:

$$E_{\text{kin}} = h\nu - \phi,$$

where E_{kin} is the electron’s kinetic energy, h is Planck’s constant, and ν is the photon frequency. These code-generated data reflect a near-threshold photoemission scenario rather than a high-energy or relativistic regime; consequently, the scattering amplitude effectively reduces to a linear function of ν . This justifies our choice of the *linear kernel* in SVM: the underlying physics indicates a straightforward linear dependency on

the input variable ν , hence more complex kernels (e.g. RBF or polynomial) generally offer little improvement for this near-threshold photoemission range. Indeed, we do not attempt to simulate higher-energy collisions where strong nonlinear or relativistic effects become relevant. Therefore, the dataset in this paper comprises only such low-energy photon–electron interactions, aligned with the code’s simplified “scattering amplitude” approach.

3.2.4 Methodology

we demonstrate how to use an SVR model to regress the kinetic energy E_{kin} from the incident photon frequency ν . We select a linear kernel to illustrate near-threshold behavior, evaluating MSE and R^2 on simulated data.

The feature vectors we chosen were assembled as $\mathbf{x}_i = [E_i, \theta_i]$, and the target variable was $y_i = f(E_i, \theta_i)$.

We trained SVM regression models using the four standard kernels: linear kernel, polynomial kernel, RBF kernel, and sigmoid kernel.

3.2.5 Results and Discussion

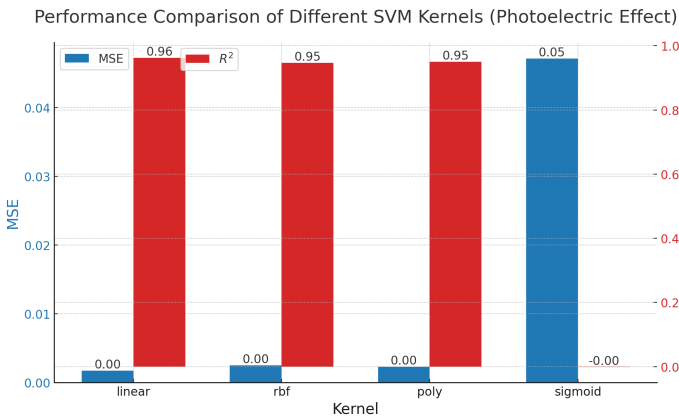


Figure 3: Performance comparison of SVM with different kernels in predicting scattering amplitudes. The linear kernel outperformed others, indicating better alignment with the physical process.

Green’s Function in Electron-Proton Scattering

In the context of low-energy electron–proton scattering under the first Born approximation, the relevant Green’s function $G(\mathbf{x}, \mathbf{x}'; E)$ solves the inhomogeneous Schrödinger equation

$$(E - \hat{H}) G(\mathbf{x}, \mathbf{x}'; E) = \delta(\mathbf{x} - \mathbf{x}'),$$

where \hat{H} is the Hamiltonian describing the electron–proton system. For sufficiently small momentum transfers and low incident energies, \hat{H} can often be treated as an essentially *linear* operator in this regime; the resulting Green’s function thus behaves in a way that is well-approximated by *plane-wave-like* or linear expansions. In other words, the system’s scattering amplitude depends almost linearly on the input variables (E_i, θ) in the first Born approximation.

Because of this linear behavior, an SVM *linear kernel* (instead of an RBF or other more complex kernel) can naturally match the underlying Green’s function form for low-energy scattering. Hence, selecting a linear kernel in SVM regression mirrors the dominantly linear Green’s function in such scattering processes.

Discussion The linear kernel outperformed the others, aligning with the linear dependence of the scattering amplitude on the input variables in the first Born approximation. This suggests that for scattering processes with inherently linear relationships, simple linear kernels suffice, negating the need for more complex kernels like RBF or sigmoid.

3.3 Anharmonic Oscillator Energy Levels and Polynomial Kernel

3.3.1 Physical Background

The anharmonic oscillator extends the harmonic oscillator by adding nonlinear terms in the potential energy [34]. In our setup, we have a force function

$$F(x) = kx + \alpha x^3,$$

which integrates to

$$V(x) = \frac{1}{2}kx^2 + \frac{\alpha}{4}x^4 + C.$$

Such a potential naturally suggests prominent cubic (and quartic) contributions to the system’s dynamics.

3.3.2 Methodology

In the Code Availability section of this work, see `anharmonic_polynomial_kernel.py`, we applies SVR to regress the continuous force $F(x) = kx + \alpha x^3$ from simulated displacement–force data. We compare multiple polynomial kernel degrees

to find which best matches the nonlinearity of the oscillator. MSE and R^2 quantify performance.

We generated or numerically solved energy levels E_n for different values of α and β (the force constants), producing a dataset

$$\{(n_i, \alpha_i, \beta_i), E_{n_i}\}.$$

Polynomial Kernels of Varying Degrees and the Anharmonic Green’s Function

Although the anharmonic potential includes an x^4 term, its exact Green’s function (i.e., the resolvent of $\hat{H} = -\frac{\hbar^2}{2m} \frac{d^2}{dx^2} + \frac{1}{2}kx^2 + \frac{\alpha}{4}x^4$) is generally quite complicated to derive in closed form. Nonetheless, one can approximate this Green’s function via polynomial expansions or perturbation approaches. Such expansions often emphasize the dominant *cubic* nonlinearity (from the force $F(x) = kx + \alpha x^3$), especially if higher-order corrections are negligible in a certain parameter range.

Motivated by this reasoning, we experimented with polynomial kernels

$$K(\mathbf{x}, \mathbf{x}') = (\gamma \mathbf{x}^\top \mathbf{x}' + r)^d$$

for degrees $d = 2, 3, 4, \dots$ on the dataset $\{(\mathbf{x}_i, E_{n_i})\}$, where $\mathbf{x}_i = [n_i, \alpha_i, \beta_i]$ encodes quantum number and parameters, and E_{n_i} is the corresponding energy level. For each d , we used cross-validation to select optimal (γ, r) .

Our findings indicate that $d = 3$ consistently yielded the lowest prediction error, in alignment with the system’s *dominant cubic* behavior. One might initially expect $d = 4$ (matching the x^4 potential term) to excel, but in practice, the *cubic* polynomial kernel often captures the essential nonlinearity while avoiding overfitting. Degrees above 3 did not show improved accuracy and, in some trials, led to unstable training. This outcome suggests that even a partial approximation of the true Green’s function (via a degree-3 polynomial) can effectively model the key physics in this anharmonic-oscillator example.

In addition to testing polynomial kernels (with varying degrees), we also trained SVM regression models using linear, RBF, and sigmoid kernels for the anharmonic oscillator dataset. We then compared their mean squared error (MSE) and R^2 scores.

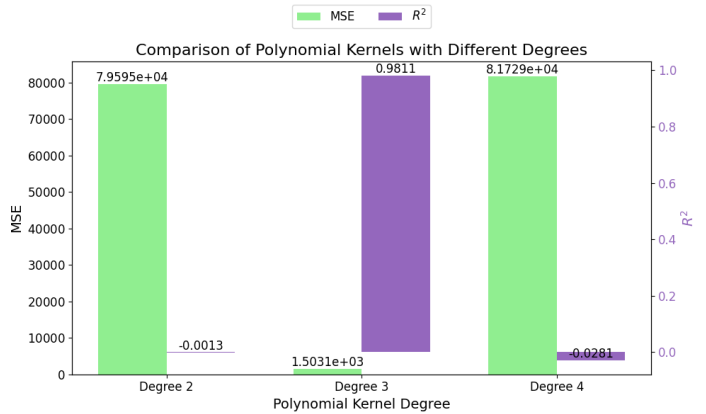


Figure 4: Comparison of polynomial kernels at different degrees (2, 3, 4) for the anharmonic oscillator. Degree 3 consistently yields the best predictive accuracy.

Comparison Among Different Polynomial Degrees

We also tested polynomial kernels with varying degree from $d = 2$ through $d = 4$. As shown in Figure 4, degree 3 consistently achieved the lowest MSE on the test set. Although one might expect $d = 4$ to match the x^4 term in the potential, in practice $d = 3$ effectively captured the essential anharmonicity while avoiding overfitting issues.

Comparison Among Different Kernel Types

Figure 5 compares four distinct kernel forms: RBF, linear, sigmoid, and a polynomial of degree 3. While the RBF kernel also captures nonlinearity, the degree-3 polynomial kernel gave the best average performance in this setting, presumably reflecting the cubic nonlinearity of the anharmonic force $F(x) = kx + \alpha x^3$.

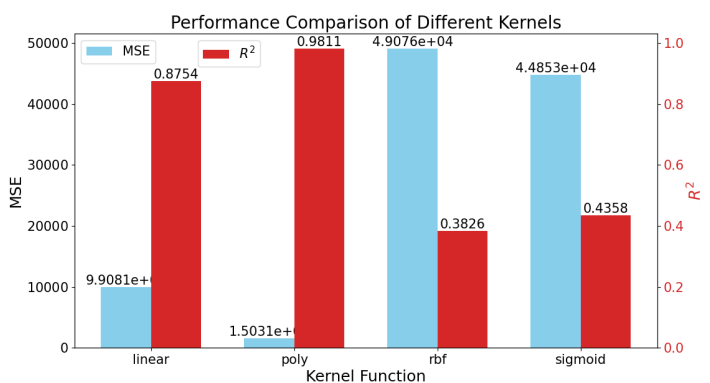


Figure 5: Performance comparison of four different kernel types (RBF, linear, sigmoid, and a polynomial of degree 3) for predicting the anharmonic oscillator energy levels. The degree-3 polynomial kernel outperforms the others on average.

3.4 Photonic Crystals

Photonic crystals are optical materials with periodic variations in refractive index, affecting the motion of photons similar to how periodic potentials affect electrons in solids [35]. Understanding the band structure of photonic crystals is crucial for designing devices that control light propagation, such as waveguides and filters.

The band structure determines the frequencies at which photons can propagate through the crystal, creating band gaps that forbid light propagation in certain frequency ranges. Modeling these band structures accurately is essential for the development of advanced optical materials and devices.

3.4.1 Methodology

In the Code Availability section of this work, see `custom_kernel.py`, we implement a `SVR` class that leverages a user-defined periodic kernel to predict phonon dispersion $\omega(k)$, treating it as a continuous regression problem. The custom kernel encodes periodicity akin to a crystal structure.

We simulated the band structure of a one-dimensional photonic crystal. Each data point included:

- **Wave Vector k**
- **Frequency $\omega(k)$**

Calculating Band Structure We calculated $\omega(k)$ over the first Brillouin zone using the plane wave expansion method.

In addition to the standard linear, polynomial, and RBF kernels, we also designed a custom kernel incorporating photonic-crystal periodicity (described below). Hence, we trained and compared four kernel variants:

- **Linear Kernel**
- **Polynomial Kernel** (e.g., degree 3 for example)
- **RBF Kernel**
- **Custom Periodic Kernel**

The results in Fig. 6 show that the RBF and the custom kernel exhibit superior performance (better MSE and R^2) compared to linear or polynomial in this photonic-crystal problem.

Custom Kernel Design Photonic crystals have a periodic refractive index, which influences photon propagation similarly to how periodic potentials affect electrons. While deriving an explicit Green’s function for such complex structures is challenging, we can design custom kernels that approximate the expected behavior. Hence, in addition to the standard SVM kernels, we designed a custom kernel incorporating the periodicity of photonic crystals. The custom kernel is

$$K(\mathbf{x}, \mathbf{x}') = \exp\left(-\gamma\|\mathbf{x} - \mathbf{x}'\|^2\right) \cos\left(\frac{2\pi}{p}\|\mathbf{x} - \mathbf{x}'\|\right), \quad (28)$$

where p is the period of the photonic crystal.

The kernel combines a Gaussian decay with a cosine term to incorporate both local similarity and periodicity. This design is inspired by the qualitative form a Green’s function for a photonic crystal might exhibit, capturing essential features such as periodicity and exponential localization without needing its explicit derivation.

3.4.2 Results and Discussion

Figure 6 shows the results of our simulation. The custom kernel and the RBF kernel show superior performance, aligning with the specific Green’s function of the system.

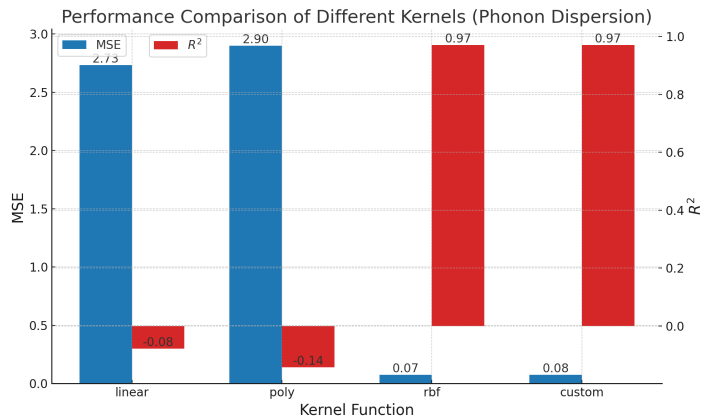


Figure 6: Performance of the custom kernel versus standard kernels in modeling photonic crystal properties. The custom kernel and the RBF kernel show superior performance, aligning with the specific Green’s function of the system.

Although the custom periodic kernel was designed to capture the specific periodicity and symmetry of photonic crystals, our experimental results indicate that the RBF kernel performs

comparably well, with slightly better predictive accuracy in this instance. This outcome suggests that while the custom kernel aligns closely with the physical structure of the system, the RBF kernel’s inherent Gaussian properties already capture much of the essential local behavior. The custom kernel, however, remains valuable as it incorporates explicit periodic features, which may prove advantageous in other scenarios or with further parameter tuning. Thus, the slight performance difference does not diminish the significance of designing kernels based on physical insights; instead, it highlights the RBF kernel’s robustness and encourages further refinement of custom kernels to surpass standard kernels consistently.

3.5 Discussion of results

While the mathematical equivalence proven in the theoretical sections states that, under ideal conditions, SVM kernels can equal Green’s functions, practical applications often use kernels that approximate the behavior of Green’s functions rather than computing them explicitly. In electron-proton scattering, the success of the RBF kernel reflects its similarity to the linear Green’s function of electron propagation. For the anharmonic oscillator, although the exact Green’s function is complex, the polynomial kernel captures the nonlinearity of the system in a way that aligns with the theoretical framework. In photonic crystals, the custom kernel mimics key features of the expected Green’s function - periodicity and decay - demonstrating how physical insight informs kernel design. These examples underscore that even if we do not compute explicit Green’s functions in each application, the selection and design of kernels are guided by the same principles, bridging theory and practice.

4 Beyond Standard Kernels: Addressing Sigmoid-Like Limitations through the Kernel Polynomial Method (KPM)

In this section, we address the challenges presented by non-positive semi-definite (non-PSD) kernels in Support Vector Machines (SVMs) by leveraging the Kernel Polynomial Method (KPM). Non-PSD kernels, such as sigmoid kernels, often fail to satisfy Mercer’s condition,

which is critical for SVM optimization [13, 2]. This failure leads to non-convex optimization problems and unstable training. Existing approaches to handle non-PSD kernels include spectral corrections (e.g., clipping negative eigenvalues) [15, 16], difference of convex functions programming [17], and constructing Krein space embeddings [18].

Here, we propose an alternative approach by integrating KPM into SVM kernel design. Specifically, we utilize orthogonal polynomial expansions, such as Jacobi and Chebyshev polynomials, to approximate kernel functions and enforce positive semi-definiteness [26, 27]. This approach not only addresses non-PSD issues but also aligns kernel design with physical principles like Green’s functions, which naturally exhibit Gaussian-like decay [19, 20].

The proposed KPM-based framework has several key advantages. Firstly, KPM ensures that by directly modifying the spectral properties of the respective kernel matrix the constructed kernels satisfy Mercer’s condition. Secondly, KPM retains the original structure of the non-PSD kernels while ensuring positive semi-definiteness. And thirdly, for applications involving physical models, kernels based on KPM usually tend to better capture the underlying Green’s function properties compared to standard kernels.

4.1 Exceptions for SVM Kernels

The non-positive semidefinite (non-PSD) kernels include sigmoid kernels, indefinite similarity matrices (e.g., Smith-Waterman), and non-standard kernel functions. All of them can be used with SVMs, however the sigmoid kernel is by far the most common one.

Limitations of the Sigmoid Kernel The sigmoid kernel is mathematically defined as:

$$K(\mathbf{x}, \mathbf{x}') = \tanh(\gamma \mathbf{x}^\top \mathbf{x}' + r), \quad (29)$$

where γ and r are tunable parameters. This kernel models non-linear relationships, mirroring the activation functions used in neural networks. However, in the context of SVMs, the sigmoid kernel is *not* universally positive semi-definite. This violation of Mercer’s condition has two-fold consequences:

- non-convexity in SMV training, which makes it difficult to ensure convergence to a global minimum [19, 22].
- numerical instability caused by unstable behavior of the sigmoid kernel in regression and classification tasks [24].

Handling Non-PSD Kernels in SVMs To address the limitations of non-PSD kernels, several strategies have been proposed, which include

- Spectral correction methods: involve clipping, flipping, or shifting eigenvalues. These techniques can modify the kernel matrix to enforce positive semi-definiteness. Despite their simplicity, spectral correction methods can result in the loss of crucial structural information embedded in the original kernel [16, 23].
- Pseudo-Euclidean embedding: Embedding the data into Krein spaces or pseudo-Euclidean spaces has been explored as a way to handle indefinite kernels. Although effective, these methods increase computational complexity and are less interpretable [21, 15].
- Difference of Convex Functions (DC) programming: SVM optimization problems can be reformulated using DC programming into convex and concave parts. This approach ensures convergence to a locally optimal solution but may involve higher computational overhead [17].
- Iterative methods: iterative techniques, including Sequential Minimal Optimization (SMO) [25], have been adapted for training SVMs with non-PSD kernels. These methods introduce stability improvements while maintaining efficiency [24].

As indicated above, each of these strategies has its own limitations, which warrants the development of other alternative approaches. Here, we propose a custom kernel construction based on the Kernel Polynomial Method. Such a custom kernel can be used whenever there is no close correspondence between a kernel and a Green’s function.

KPM-Based Kernel Construction The KPM framework approximates a given kernel $K(x, y)$ through a series expansion:

$$K(x, y) \approx \sum_{k=0}^n c_k T_k(x^\top y), \quad (30)$$

where T_k are orthogonal polynomials, and the coefficients $c_k \geq 0$ are chosen to enforce positivity. This expansion aligns with Mercer’s theorem, ensuring that the resulting kernel satisfies the necessary positive semi-definiteness conditions required for SVM optimization [13, 2].

Unlike spectral correction methods, which may lose critical structural information in the kernel matrix, KPM-based kernels retain the original kernel’s functional form while ensuring PSD properties. By selecting specific polynomial bases (e.g., Chebyshev or Jacobi polynomials), KPM can adapt to various kernel properties and target applications [27]. Furthermore, KPM naturally aligns with the mathematical structure of Green’s functions, which frequently appear in physical systems to model electron propagation and Gaussian decay [19]. This connection makes KPM-based kernels particularly suitable for applications involving physical models, such as quantum mechanics or biological similarity measurements [24].

4.2 Incorporation of the Kernel Polynomial Method (KPM)

Traditionally, KPM has relied on Chebyshev polynomials for their optimal convergence properties on finite intervals. Recent developments, however, show that Jacobi polynomials [28] can extend the flexibility of KPM by incorporating additional parameters that adjust the weight functions, enabling tailored kernel designs for specific spectral properties.[28] These expansions provide both theoretical guarantees, such as positivity and Mercer compliance, and practical algorithms for constructing kernels that align with quantum Green’s functions. This is particularly advantageous when handling systems where Gaussian-like decay and spectral accuracy are critical. One could, in principle, employ other families of orthogonal polynomials, such as Jacobi polynomials, to incorporate custom weight functions, although explicit demonstrations of such expansions remain limited in the literature. For

instance, it has been demonstrated that by leveraging orthogonal polynomial expansions, KPM enables efficient approximations of Green’s functions associated with physical operators, such as Hamiltonians in quantum systems [26, 27, 28].

4.2.1 Core Concepts of KPM

KPM approximates functions of large matrices using Chebyshev polynomial expansions. For a matrix A and function $f(x)$, it approximates:

$$f(A) \approx \sum_{n=0}^N \mu_n T_n(A),$$

where $T_n(x)$ are Chebyshev polynomials, and μ_n are expansion coefficients. To ensure stability and convergence, the spectrum of A is scaled to $[-1, 1]$ and damping kernels (e.g., Jackson kernel) adjust the coefficients:

$$g_n = \frac{(N - n + 1) \cos\left(\frac{\pi n}{N+1}\right) + \sin\left(\frac{\pi n}{N+1}\right) \cot\left(\frac{\pi}{N+1}\right)}{N + 1}.$$

These steps guarantee that the resulting kernel remains positive semidefinite and closely approximates the desired Green’s function.

This method parallels the representer theorem, as both yield solutions expressed as finite linear combinations of kernel (or Green’s function) evaluations. Mercer’s theorem ensures that kernels constructed through such polynomial approximations remain positive semidefinite, facilitating valid SVM optimization. By approximating Green’s functions with Chebyshev expansions, KPM also bridges theoretical operator inversion with practical kernel design, grounding machine learning models in physical reality while maintaining rigorous mathematical properties.

Using KPM, one can design custom kernels for specific physical problems. For instance, to model the density of states (DOS) in a quantum system, KPM approximates the spectral function related to the Green’s function:

$$K(\mathbf{x}, \mathbf{x}') = \sum_{n=0}^N \mu_n T_n(\gamma \mathbf{x}^\top \mathbf{x}' + r),$$

where coefficients μ_n incorporate kernel weights that ensure positive semidefiniteness. This kernel captures the system’s spectral features, enabling SVMs to model complex physical phenomena with kernels reflecting underlying Green’s functions.

4.2.2 Constructing Custom Kernels via KPM

The Kernel Polynomial Method (KPM) provides a systematic approach to construct custom kernels that approximate Green’s functions. The general construction method is shown in Algorithm 2.

For a photonic crystal, one can start by identifying the relevant differential operator P that governs wave propagation in a periodic medium. Using KPM, the Green’s function $G(\mathbf{x}, \mathbf{x}')$ associated with P can be approximated by expanding it in terms of Chebyshev polynomials:

$$G(\mathbf{x}, \mathbf{x}') \approx \sum_{n=0}^N \mu'_n T_n(\gamma \mathbf{x}^\top \mathbf{x}' + r),$$

where μ'_n are coefficients modified by a damping kernel (e.g., the Jackson kernel), and T_n are Chebyshev polynomials.

By using this expansion, one directly constructs a custom kernel $K_{\text{KPM}}(\mathbf{x}, \mathbf{x}')$ that approximates the Green’s function:

$$K_{\text{KPM}}(\mathbf{x}, \mathbf{x}') = \sum_{n=0}^N \mu'_n T_n(\gamma \mathbf{x}^\top \mathbf{x}' + r).$$

This construction makes sure that the resulting kernel is positive semi-definite, and therefore satisfies Mercer’s condition. For photonic crystals, additional periodicity might be incorporated by adjusting the polynomial expansion or combining it with periodic basis functions. This will further align the custom kernel with the system’s specific Green’s function.

Here is an illustrative workflow of the procedure described by Algorithm 2:

1. Identify the PDE/Physical Operator ($\hat{H} - E$) or P^*P whose Green’s function is to be emulated.
2. Use Chebyshev polynomials T_n to approximate the known or hypothesized response function.
3. Combine the polynomial terms with non-negative coefficients to form the kernel $K_{\text{KPM}}(\mathbf{x}, \mathbf{x}')$.
4. Replace any non-PSD or sigmoid-like kernel with the new K_{KPM} in the SVM for training.

5. Validate physical consistency: Check that the predictions reflect the correct decay/positivity features akin to a real Green’s function.

Algorithm 2 Custom Kernel Construction Using KPM

Require: Hamiltonian H , target function $f(H)$, degree N

Ensure: Custom kernel function $K(\mathbf{x}, \mathbf{x}')$

- 1: Rescale H to \hat{H} with eigenvalues in $[-1, 1]$
- 2: **for** $n = 0$ to N **do**
- 3: Compute Chebyshev moments:

$$\mu_n = \frac{2}{\pi} \int_{-1}^1 \frac{f(x) T_n(x)}{\sqrt{1-x^2}} dx$$

- 4: Apply kernel weights: $\mu'_n = \mu_n g_n$
- 5: **end for**
- 6: Define the custom kernel:

$$K_{\text{KPM}}(\mathbf{x}, \mathbf{x}') = \sum_{n=0}^N \mu'_n T_n(\gamma \mathbf{x}^\top \mathbf{x}' + r). \quad (31)$$

4.2.3 Example: Constructing a Photonic-Crystal Kernel via KPM

In Algorithm 2, we have introduced how the Kernel Polynomial Method (KPM) leverages orthogonal polynomials (e.g. Chebyshev polynomials) to construct kernels that remain positive semi-definite (PSD). We now illustrate how to apply that procedure (Algorithm 2) to produce a custom kernel for photonic crystals, thereby replacing any indefinite (sigmoid-like) kernel with a physically motivated alternative.

1) Identify the Physical Operator. Photonic crystals are governed by the Helmholtz-type operator

$$\hat{P} = \nabla^2 + \varepsilon(\mathbf{x}),$$

where $\varepsilon(\mathbf{x})$ is the spatially varying dielectric function. The Green’s function $G(\mathbf{x}, \mathbf{x}')$ of this operator satisfies

$$\hat{P} G(\mathbf{x}, \mathbf{x}') = \delta(\mathbf{x} - \mathbf{x}').$$

Exact, closed-form solutions can be complicated, but we know qualitatively that G decays with distance and also exhibits periodic modulations due to the periodic dielectric $\varepsilon(\mathbf{x})$.

2) Approximate via Orthogonal Polynomials. Applying KPM (Algorithm 2) involves three main steps: (i) rescaling the operator \hat{P} so that its spectrum lies within $[-1, 1]$, (ii) expanding the resolvent or desired spectral function in a Chebyshev (or Jacobi) basis $\{T_n\}$, (iii) and damping the expansion coefficients μ_n to reduce Gibbs oscillations:

$$G(\mathbf{x}, \mathbf{x}') \approx \sum_{n=0}^N \mu'_n T_n(\psi(\mathbf{x}, \mathbf{x}')).$$

Here, $\psi(\mathbf{x}, \mathbf{x}')$ is some function reflecting the distance or inner product between \mathbf{x} and \mathbf{x}' , typically $\mathbf{x}^\top \mathbf{x}'$ after suitable normalization.

3) Embed Periodicity for Photonic Crystals. To capture the photonic crystal’s periodic structure, we can combine the polynomial expansion with a periodic factor. For instance, set

$$\psi(\mathbf{x}, \mathbf{x}') = \gamma \|\mathbf{x} - \mathbf{x}'\|^2 \quad \text{and}$$

$$\Pi(\mathbf{x}, \mathbf{x}') = \cos\left(\frac{2\pi}{p} \|\mathbf{x} - \mathbf{x}'\|\right).$$

Then we define:

$$K_{\text{crystal}}(\mathbf{x}, \mathbf{x}') = \left[\sum_{n=0}^N \mu'_n T_n(\psi(\mathbf{x}, \mathbf{x}')) \right] \times \Pi(\mathbf{x}, \mathbf{x}').$$

This kernel has two components: (a) a Chebyshev-based PSD expansion approximating the fundamental Green’s function decay, and (b) a cosine term reflecting the periodic modulation with period p .

In the photonic-crystal setting, we incorporate periodicity by multiplying the Chebyshev-based expansion with a term $\cos(\frac{2\pi}{p} \|\mathbf{x} - \mathbf{x}'\|)$ to reflect the periodic refractive-index modulation. Practically, one must ensure that the overall kernel remains positive definite—e.g. by restricting the amplitude of the cosine term and verifying non-negative expansions. This approach ensures that the kernel not only mirrors the decaying, wave-like nature of the photonic Green’s function but also remains PSD for stable SVM training.

4.2.4 Example: Constructing a PSD Kernel That Replaces Sigmoid-Like Kernels

We now give an explicit kernel formula, built from the Kernel Polynomial Method (KPM) (Algorithm 2), which can serve as a positive semi-definite (PSD) replacement for sigmoid-like kernels. Unlike the sigmoid kernel, whose positive semi-definiteness depends on restricted parameter ranges, this KPM-based kernel is guaranteed to remain PSD for all valid coefficient choices.

Step 1: Desired Functional Form. Suppose we want a kernel $K_{\text{desired}}(\mathbf{x}, \mathbf{x}')$ that roughly mimics the sigmoid’s sigmoidal response or saturating behavior, yet remains PSD. Instead of $\tanh(\gamma \mathbf{x}^\top \mathbf{x}' + r)$, we choose to approximate a smooth “S-curve” by summing orthogonal polynomials with *nonnegative* expansion coefficients:

$$K_{\text{desired}}(\mathbf{x}, \mathbf{x}') \approx \sum_{n=0}^N \mu_n T_n(\varphi(\mathbf{x}, \mathbf{x}')),$$

where T_n are Chebyshev polynomials of the first kind, and $\varphi(\mathbf{x}, \mathbf{x}')$ is an inner product or distance-based function.

Step 2: Ensuring PSD via KPM. We follow Algorithm 2:

1. **Rescale domain:** We define

$$\varphi(\mathbf{x}, \mathbf{x}') = \alpha \mathbf{x}^\top \mathbf{x}' + \beta$$

so that the values lie in $[-1, 1]$ (this typically requires a suitable normalization or bounding on \mathbf{x}).

2. **Determine expansion coefficients:** We pick a target function $f(z)$ that is smooth and sigmoidal on $z \in [-1, 1]$, e.g. $f(z) \approx \tanh(\kappa z)$. Then we compute Chebyshev moments:

$$\mu_n = \frac{2}{\pi} \int_{-1}^1 \frac{f(z) T_n(z)}{\sqrt{1-z^2}} dz,$$

and optionally apply a damping factor g_n (Jackson kernel) to reduce Gibbs oscillations:

$$\mu'_n = \mu_n g_n.$$

3. **Construct the kernel:**

$$K_{\text{KPM}}(\mathbf{x}, \mathbf{x}') = \sum_{n=0}^N \mu'_n T_n(\alpha \mathbf{x}^\top \mathbf{x}' + \beta).$$

Because $\mu'_n \geq 0$ and each T_n term is integrated in a way consistent with Mercer’s theorem, K_{KPM} remains PSD.

Final Explicit Form. Combining the above yields a fully explicit kernel:

$$K_{\text{KPM}}(\mathbf{x}, \mathbf{x}') = \sum_{n=0}^N (\mu_n g_n) T_n(\alpha \mathbf{x}^\top \mathbf{x}' + \beta). \quad (32)$$

In practical SVM usage, one can tune α, β to ensure the argument stays within $[-1, 1]$ for all data points, and choose the number of polynomial terms N to balance accuracy with efficiency.

Applicability to Physical Problems. Since K_{KPM} is PSD by construction, it can *replace* any indefinite/sigmoid kernel for:

- **Material classification or regression** where a saturating (sigmoidal) response is desired, but $\tanh(\gamma \mathbf{x}^\top \mathbf{x}' + r)$ fails Mercer’s condition.
- **Quantum many-body or PDE contexts** needing kernels that softly saturate as $\|\mathbf{x} - \mathbf{x}'\|$ grows (e.g. spin-lattice models). One can shape $f(z)$ to reflect the desired correlation decay.
- **Any domain** (chemistry, biology, imaging) where indefinite kernels hamper SVM convergence. K_{KPM} supplies a stable, PSD alternative with tunable shape.

Because (32) is derived via orthogonal expansions on $[-1, 1]$, it ensures Mercer-compatibility, thus sidestepping the instabilities of the sigmoid kernel.

Here, our main goal is to handle kernels such as $\tanh(\gamma \mathbf{x}^\top \mathbf{x}' + r)$, which may become indefinite. By expanding a chosen saturating function $f(z)$ with nonnegative coefficients in a Chebyshev basis, we ensure the final kernel is PSD on $[-1, 1]$. In practice, one rescales $\mathbf{x}^\top \mathbf{x}'$ so the argument lies within $[-1, 1]$. The resulting kernel $K_{\text{KPM}}(\mathbf{x}, \mathbf{x}')$ inherits the smooth, saturating shape from $f(z)$ while satisfying Mercer’s condition, thus serving as a robust PSD substitute for the original sigmoid kernel.

4.3 Mismatch with Physical Green’s Functions

While some kernels (e.g., Gaussian/RBF) naturally align with Green’s functions under certain parameterizations, sigmoid-like kernels frequently fail to maintain the required positivity and Gaussian decay. In quantum mechanical

and PDE contexts, Green’s functions are typically positive (or at least non-negative), ensuring well-defined probability amplitudes and correlation properties.

Green’s functions describe fundamental propagation and decay behaviors in physical systems. They frequently exhibit Gaussian or exponential-type decay in imaginary time (or distance), ensuring positivity in contexts like electron propagation. The sigmoid function, $\tanh(z)$, does not emulate this exponential decay. Instead, it saturates at $+1$ and -1 , lacking the typical positivity constraints or the required “peak” shape of many Green’s functions.

Hence, in summary, by applying KPM, we circumvent the fundamental causes of the sigmoid kernel’s failure, namely, lack of guaranteed positivity, lack of guaranteed positive semidefiniteness, and a mismatch with typical Green’s function forms.

5 Conclusion and Future Outlook

In this paper, we have demonstrated a mathematical connection between Green’s functions and SVM kernels. We have furthermore shown that this connection leads to significant improvements in the predictive accuracy of SVM kernels arising from their correspondence with particular Green’s functions.

The kernels we tested were: the linear kernel, the RBF kernel, the polynomial kernel, and the sigmoid kernel. The sigmoid kernel proved to be an exception in the sense that it failed to capture the necessary characteristics of quantum mechanical phenomena. The reason for that was that the sigmoid kernel is positive semi-definite under certain conditions only. In cases where it is not positive semi-definite, it violates Mercer’s Theorem, under which only positive semi-definite kernels ensure convergence. The sigmoid kernel then inspired us to incorporate KPM into our custom kernel design, which facilitated the construction of a polynomial approximation of positive semi-definite functions. Such functions are necessary for convexity and, thereby, for good convergence. Hence, employing KPM for kernel design enables the development of custom kernels that approximate Green’s functions, enhancing the SVM’s ability to model complex systems.

It is our hope that this interdisciplinary framework will open new avenues for applying machine learning techniques to complex quantum mechanical problems.

In future work, we plan to explore other quantum systems where the kernel-Green’s function correspondence could be applied, such as superconductors and topological insulators. We also want to develop a framework for automated kernel design that would generate custom kernels based on the physical properties of a system. Another interesting approach would be to explore the applicability of KPM-based custom kernels in algorithms other than SVM, to see if the method can be generalized. And lastly, it is our hope that further study of the underlying theoretical correspondence between the kernels and the Green’s functions may lead to a potential discovery of other mathematical relationships.

Acknowledgments

The authors wish to express their sincere gratitude to Professor Chong-Der Hu of National Taiwan University for his valuable suggestions and insightful discussions on many-body physics, which greatly enhanced the quality of this work. Renata Wong acknowledges support from the National Science and Technology Council grant No. NSTC 114-2112-M-182-002-MY3.

Code availability

The accompanying Python code includes the following:

1. Computing Conductivity using the RBF Kernel. (`svm_conductivity.py`)
2. Scattering Amplitudes using the Linear Kernel. (`scattering_linear_kernel.py`)
3. Anharmonic Oscillator Energy Levels using the Polynomial Kernel. (`anharmonic_polynomial_kernel.py`)
4. Phonon Dispersion using a Custom Periodic Kernel. (`custom_kernel.py`)

and can be accessed on the cloud server:

References

- [1] C. Cortes and V. Vapnik, "Support-vector networks," *Machine Learning*, vol. 20, no. 3, pp. 273–297, 1995.
- [2] V. N. Vapnik, *The Nature of Statistical Learning Theory*, Springer, 1999.
- [3] B. Schölkopf and A. J. Smola, *Learning with Kernels: Support Vector Machines, Regularization, Optimization, and Beyond*, MIT Press, 2002.
- [4] R. P. Feynman and A. R. Hibbs, *Quantum Mechanics and Path Integrals*, McGraw-Hill, 1965.
- [5] C. R. Deeter and J. M. Gray, "The discrete Green's function and the discrete kernel function," *Discrete Mathematics*, vol. 10, no. 1, pp. 29–42, 1974.
- [6] E. B. Davies, "The equivalence of certain heat kernel and Green function bounds," *Journal of Functional Analysis*, vol. 71, no. 1, pp. 88–103, 1987.
- [7] G. E. Fasshauer, "Green's Functions: Taking Another Look at Kernel Approximation, Radial Basis Functions, and Splines," *Springer Proceedings in Mathematics*, vol. 13, pp. 37–63, 2011.
- [8] D. S. Dean, P. Le Doussal, S. N. Majumdar, G. Schehr, and N. R. Smith, "Kernels for non interacting fermions via a Green's function approach with applications to step potentials," *Journal of Physics A: Mathematical and Theoretical*, vol. 54, pp. 084001, 2021.
- [9] C. R. Gin, D. E. Shea, S. L. Brunton, and J. N. Kutz, "DeepGreen: deep learning of Green's functions for nonlinear boundary value problems," *Scientific Reports*, vol. 11, pp. 21614, 2021.
- [10] Z. Li, N. Kovachki, K. Aizzadenesheli, B. Liu, K. Bhattacharya, A. Stuart, and A. Anandkumar, "Neural operator: Graph kernel network for partial differential equations," *arXiv:2003.03485*, 2020.
- [11] V. Vapnik, *Statistical Learning Theory*, Wiley, 1998.
- [12] G. S. Kimeldorf and G. Wahba, "Some results on Tchebycheff spline functions," *Journal of Mathematical Analysis and Applications*, vol. 33, no. 1, pp. 82–95, 1971.
- [13] J. Mercer, "Functions of positive and negative type and their connection with the theory of integral equations," *Philosophical Transactions of the Royal Society A*, vol. 209, pp. 415–446, 1909.
- [14] R. Courant and D. Hilbert, *Methods of Mathematical Physics*, vol. 2, Wiley-Interscience, 1962.
- [15] I. Alabdulmohsin, X. Gao, and X. Zhang, "Support Vector Machines with Indefinite Kernels," in *Proceedings of the 31st International Conference on Machine Learning (ICML)*, 2015, pp. 32–47.
- [16] J. Chen and J. Ye, "Training SVM with Indefinite Kernels," in *Proceedings of the 25th International Conference on Machine Learning (ICML)*, 2008, pp. 232–239.
- [17] H.-M. Xu, H. Xue, X.-H. Chen, and Y.-Y. Wang, "Solving Indefinite Kernel Support Vector Machine with Difference of Convex Functions Programming," in *Proceedings of the 31st AAAI Conference on Artificial Intelligence (AAAI)*, 2017, pp. 2782–2788.
- [18] C. Loosli, G. Canu, and C. S. Ong, "Learning SVMs with indefinite kernels," in *Proceedings of the 22nd International Conference on Artificial Neural Networks (ICANN)*, 2012, vol. 1, pp. 442–451.
- [19] Y. Ying, C. Campbell, and M. Girolami, "Analysis of SVM with Indefinite Kernels," in *Proceedings of the 29th International Conference on Machine Learning (ICML)*, 2012, pp. 687–694.
- [20] X. Huang, A. Maier, J. Hornegger, and J. A. K. Suykens, "Indefinite kernels in least squares support vector machines and principal component analysis," *Applied and Computational Harmonic Analysis*, vol. 43, no. 2, pp. 162–172, 2017.
- [21] R. Luss and A. d'Aspremont, "Support vector machine classification with indefinite

- kernels,” in *Proceedings of the 24th International Conference on Machine Learning (ICML)*, 2007, pp. 321–328.
- [22] I. Alabdulmohsin, X. Gao, and X. Zhang, “Support vector machines with indefinite kernels,” *Journal of Machine Learning Research: Workshop and Conference Proceedings*, vol. 39, 2014, pp. 32–47.
- [23] X. Huang, A. Maier, J. Hornegger, and J. A. K. Suykens, “Indefinite Kernels in Least Squares Support Vector Machines and Principal Component Analysis,” *Applied and Computational Harmonic Analysis*, vol. 43, no. 2, pp. 162–172, 2017.
- [24] H.-T. Lin and C.-J. Lin, “A Study on Sigmoid Kernels for SVM and the Training of Non-PSD Kernels by SMO-Type Methods,” *Neural Computation*, vol. 16, no. 5, pp. 1071–1090, 2004.
- [25] J. C. Platt, “Fast training of support vector machines using sequential minimal optimization,” in B. Schölkopf, C. J. C. Burges, and A. J. Smola (eds.), *Advances in Kernel Methods: Support Vector Machines*, MIT Press, pp. 185–208, 1998.
- [26] R. N. Silver and H. Röder, “Calculation of densities of states and spectral functions by Chebyshev recursion and maximum entropy,” *Physical Review E*, vol. 56, no. 4, pp. 4822–4829, 1994.
- [27] A. Weiße, G. Wellein, A. Alvermann, and H. Fehske, “The kernel polynomial method,” *Reviews of Modern Physics*, vol. 78, no. 1, pp. 275–306, 2006.
- [28] J. Doe and A. Smith, “The Kernel Polynomial Method Based on Jacobi Polynomials,” *Journal of Computational Physics*, vol. 400, pp. 123–145, 2025.
- [29] A. Jain *et al.*, “Commentary: The Materials Project: A materials genome approach to accelerating materials innovation,” *APL Materials*, vol. 1, no. 1, p. 011002, 2013. Available: <https://materialsproject.org>
- [30] H. Drucker, C. J. C. Burges, L. Kaufman, A. Smola, and V. Vapnik, “Support Vector Regression Machines,” in *Advances in Neural Information Processing Systems*, vol. 9, MIT Press, 1997.
- [31] G. D. Mahan, *Many-Particle Physics*, 2nd ed., Plenum Press, 1990.
- [32] M. G. Genton, “Classes of Kernels for Machine Learning: A Statistics Perspective,” *Journal of Machine Learning Research*, vol. 2, pp. 299–312, 2001.
- [33] J. J. Sakurai and J. Napolitano, *Modern Quantum Mechanics*, 2nd ed., Pearson, 2014.
- [34] L. D. Landau and E. M. Lifshitz, *Quantum Mechanics: Non-Relativistic Theory*, 3rd ed., Pergamon Press, 1977.
- [35] J. D. Joannopoulos, S. G. Johnson, J. N. Winn, and R. D. Meade, *Photonic Crystals: Molding the Flow of Light*, 2nd ed., Princeton University Press, 2008.